CHAPTER II

EXPERIMENTAL SECTION

2.1 Materials

The experiments were carried out using linear low density polyethylenes (LLDPE). LLDPE's used in this study were L1810F, L2009F and L2020F which were of the film grade, supplied by Thai Polyethylene Co., Ltd. The materials were in pellet form with their properties shown below :

Table 2.1 Physical properties of LLDPE

Physical Properties	L1810F	L2009F	L2020F
MFI (g/10min.)	0.9110 ± 0.0061	0.9770 ± 0.0034	1.7770± 0.0027
M_W (g/mol)	$1.27x10^5$	$1.03x10^5$	$6.07x10^4$
% Crystallinity	34.79	36.63	34.82
T_m (°c)	128.5	129.4	130.5
Density (g/cm^3)	0.9181	0.9186	0.9192

For the stability diagram, we had to use two samples of HDPE obtained from Naiyakul (1997) and Polnark (1997) and their properties are reported below.

Table 2.2 Physical properties of HDPE

Physical Properties	H5690S	R1760
MFI (g/10min.)	0.9	3.0
M_W (g/mol)	$1.84x10^4$	-
T_m (°c)	132.0	-
Density (g/cm^3)	0.9560	0.9570

2.2 Characterization Studies

The characterization studies were used to quantify the physical properties of the raw materials.

2.2.1 Melt Flow Index (MFI : g/10min.)

Our procedure followed ASTM 1238 standard. The MFI instrument is ZWICK model 4105 Extrusion Plastomer, with recommended temperature of 190°C and a load of 2.16 kg. for polyethylene. An average was taken for five measurements and the standard deviation was computed as shown.

2.2.2 % Crystallinity and Melting Temperature (T_m : °c)

Both properties were obtained from Differential Scanning Colorimeter (DSC), model TASC 414/3 from NETZCH (Thermiche Analyse). The temperature range was 30 - 300°C with a heating rate of 10°C/min.

2.2.3 Weight Average Molecular Weight (M_W : g/mol)

M_W was obtained from Gel Permeation Chromatography (GPC) or Side Exclusion Chromatography (SEC), model Waters 150-C at the King Mongkut Institute of Technology, Lardkrabang. Temperature was 135 °C and dichlorobenzene was used as the solvent.

2.2.4 Density (ρ : g/cm^3)

ASTM 1505 procedure was followed to obtain the density by a density gradient column. Temperature was set at 23 °C, and sodium acetate and methanol were used as mixture solvents. The services for the density measurements were provided by Thai Polyethlylene Co., Ltd. (TPE) staff.

2.3 Capillary Rheometer Studies

2.3.1 Instrument

The measurement was performed on an Instron model 3213 capillary rheometer which was designed for use with an Instron material testing system. It comprises of an extrusion assembly equipped with a plunger driven at a constant speed. A temperature control system is contained in a separate console. It incorporates these features: barrel length of 289 mm, barrel diameter of 9.525 mm, a maximum load of 25 kN, a precise temperature control from 40-400°C, temperature stability at the capillary of ± 0.5 °C.

Capillary Dies : Both of our die had a 45° tapering but of two different sizes: die no. 614 was 0.7645 mm in diameter and 22.5 mm long. It's length-to-diameter ratio was 33.4 and die no. 1855 was 1.2751 mm in diameter and 50.9 mm long. It's length-to-diameter ratio was 39.9.

2.3.2 Procedure

A sample of LLDPE to be studied was placed in the barrel of the extrusion assembly, heated to a required temperature (185°C) and then forced out through a capillary die located at the bottom of the Instron machine at a constant plunger speed. A force corresponding to a specific plunger speed can be plotted on a chart recorder. The force and the plunger speed are converted to shear stress and shear rate values by simple mathematical calculations involving the geometry of the extruder.

2.3.3 Calculations

In our calculations, we assumed that the polymer melt was incompressible, the flow was laminar and fully developed, and there was no entrance and exit loss.

■ *Determination of Wall Shear Stress (τ_w)*

The force was converted into the wall shear stress by using the following equations involving the geometry of the capillary and the plunger (Dealy,1991) :

$$\tau_w = \frac{F}{4A_p(l_c / d_c)}, \tag{2.1}$$

where F is the force or load of the plunger, A_p is the cross section area of the plunger, l_c is the length of capillary die and d_c is the diameter of capillary die. The wall shear stress is actually the apparent wall shear stress and the Bagley correction was not applied because l_c/d_c was greater than 30; the entrance and exit losses were negligible.

■ *Determination of the Apparent Strain Rate ($\dot{\gamma}_a$)*

The plunger velocity was converted into apparent strain rate by the following equation

$$\dot{\gamma}_a = 8 \times V_p \times \frac{d_b^2}{d_c^3}, \tag{2.2}$$

where V_c is the capillary velocity, V_p is the plunger velocity and d_b is a barrel diameter. The plunger velocity was converted to the capillary velocity by the equation

$$V_c = V_p\left(\frac{d_b}{d_c}\right)^2, \tag{2.3}$$

and

$$\dot{\gamma}_a = \frac{8V_c}{d_c}. \tag{2.4}$$

■ *Determination of Viscosity (η) and Power Law Index (n)*

The viscosity was determined from

$$\eta = \frac{\tau_w}{\dot{\gamma}_a}, \tag{2.5}$$

If we assume a non - Newtonian melt, it obeys the power law fluid behaviour,

$$\tau_w = K\left(\dot{\gamma}_w\right), \tag{2.6}$$

where $\dot{\gamma}_W$ is the wall strain rate, n is the power law index and K is a constant. Alternatively we can write equation (2.6) as

$$\tau_w = \eta\dot{\gamma}_w, \tag{2.7}$$

then it follows that

$$\eta = K\left(\dot{\gamma}_w\right)^{n-1}. \tag{2.8}$$

From the definition of Rabinowitz correction (Ramamurthy, 1986)

$$\dot{\gamma}_w = \frac{(3n+1)}{4n}\dot{\gamma}_{a,s}, \tag{2.9}$$

where $\dot{\gamma}_{a,S}$ is the apparent strain rate without slip. It follows that

$$\tau_w = K\left[\left(\frac{3n+1}{4n}\right)\dot{\gamma}_{a,s}\right]^n, \tag{2.10}$$

or

$$\tau_w = K\left[\left(\frac{3n+1}{4n}\right)\left(\dot{\gamma}_a - \frac{8Vs}{d_c}\right)\right]^n, \tag{2.11}$$

where V_S is the slip velocity. If we assume a small slip so $8V_S/d_C$ is much smaller than $\dot{\gamma}_a$ then,

$$\tau_w \cong K\left(\frac{3n+1}{4n}\right)^n\left(\dot{\gamma}_a\right)^n, \tag{2.12}$$

and

$$\eta \cong K\left(\frac{3n+1}{4n}\right)^n\left(\dot{\gamma}_a\right)^{n-1}. \tag{2.13}$$

So the power law index (n) and constant K can be obtained from the plot of $\log \eta$ vs. $\log \dot{\gamma}_a$.

■ *Determination of Wall Strain Rate ($\dot{\gamma}_w$) and Apparent Strain Rate without Slip ($\dot{\gamma}_{a,s}$)*

From the power law fluid of equation (2.6) we can write

$$\dot{\gamma}_w = \left(\frac{\tau_w}{K}\right)^n . \tag{2.14}$$

Using the Rabinowitz correction, we can write

$$\dot{\gamma}_{a,s} = \frac{4n}{3n+1}\left(\frac{\tau_w}{K}\right)^{1/n} . \tag{2.15}$$

■ *Determination of Slip Velocity (V_s) in the Oscillating Flow Regimes*

From the plot of load vs. plunger travel, the load fluctuates. The load becomes doubled values at a given plunger speed in the oscillating flow regimes. The difference between the maximum and minimum loads from each fluctuation is determined as

$$\Delta\tau_w = \tau_{max} - \tau_{min} , \tag{2.16}$$

where τ_{max} is a stress at the upper load in a cycle and τ_{min} is a stress at the lower load in a cycle. We assume that there was no change in the apparent viscosity of the polymer melt as the load fluctuates. Only the change in the shear stress between the upper and lower values occurs. The change of the apparent strain rate ($\Delta\dot{\gamma}_a$) can be determined as

$$\Delta\dot{\gamma}_a = \frac{\Delta\tau_w}{\eta n} , \tag{2.17}$$

where $\Delta\tau_W$ is the different in the wall shear stress between the upper and lower points of load fluctuation . The slip velocity (V_S) for each oscillation cycle is calculated from

$$V_s = \frac{\Delta\dot{\gamma}_a}{8} \times \dot{d}_c . \qquad (2.18)$$

The slip velocity of each plunger speed reported was determined by averaging the slip velocity values of 3 - 4 cycles.

■ *Determination of Load Wavelength (λ_l) in Oscillating Flow Regimes*

The load wavelength is the length between a maximum and the next maximum point or the length between a minimum and the next minimum point of the load fluctuations. The load period was calculated from

$$\Delta T = T_n - T_{n-1} , \qquad (2.19)$$

where T is the plunger travel (mm) at maximum or minimum load and n is the number of peak at the same plunger speed. The load wavelength (λ_l) was calculated from :

$$\lambda_l = \Delta T \times \left(\frac{d_b}{d_c}\right)^2 . \qquad (2.20)$$

■ *Determination of Extrudate Wavelength (λ_e) in Oscillating Flow Regimes*

The extrudate wavelength (λ_e) was determined by a visual measurement of the length of the sharkskin plus the smooth surface in one cycle of oscillation. The resolution was on a millimetre scale.

2.4 Parallel Plate Rheometer Studies

2.4.1 Instrument

Advanced Rheometric Expansion System (ARES) is a mechanical spectrometer that is capable of subjecting a sample to either a dynamic (sinusoidal) or steady (linear) shear strain (deformation). It measures the resultant torque exorted by the sample in response to the input shear strain. Shear strain is controlled by the actuator ; torque is measured by transducers.

2.4.2 Procedure

A sample was placed in the gap between the two parallel plates which was 50 mm in diameter. The measurement mode was Dynamic Frequency/Temperature Sweep. The temperature was varied between 185-115°C, the frequency was from 0.1 - 100 rad/s.. This instrument gives the value of storage modulus (G') and loss modulus (G") vs. frequency (ω).

2.4.3 Calculations

Time and Temperature Superposition master curve allows a viscoelastic behavior at one temperature to be related to that of another temperature. Because of the limiting frequency range in one temperature was too narrow, so we had to do an experiment at many temperatures and created the time and temperature superposition master curve for a wider range of frequency. We obtained shift factor from empirical measurements, by assuming the reference temperature of 185°C and measuring the horizontal shift factor (a_T), then fitting the empirical shift factor with the WLF - equation :

$$\log a_T = \frac{-C_1(T - T_o)}{C_2 + (T - T_o)}. \qquad (2.21)$$

From WLF- equation, we calculated the constant of C_1 and C_2. We then took the constant values to calculate the shift factor (log a_T) which was used to generate the time and temperature master curve. If we used only the shift factor (a_T) or the horizontal shift, the master curve would not collapse well, so we had to use the vertical shift factor (b_T)

$$b_T = \frac{T_o}{T}. \tag{2.22}$$

■ *Determination of Viscosity (η)*

The viscosity obtained from the parallel plate rheometer was determined from

$$\eta' = \frac{G''}{\omega}, \tag{2.23}$$

where G'' is the loss modulus and ω is frequency or angular velocity.

2.5 Viscosity Comparison

To compare the viscosity with that obtained from the capillary rheometer, the angular frequency (ω) of parallel plate rheometer had to be converted to the steady strain rate by the transformation :

$$\gamma_w = \frac{\omega R}{2\pi h}, \tag{2.24}$$

where ω is frequency or angular velocity, R is radius of the plate and h is gap spacing.

Without Begley correction, the viscosity in capillary rheometer should be more than the viscosity in the parallel plate rheometer but figures 2.1(a), 2.2(a) and 2.3(a) show that the parallel plate rheometer gives a higher viscosity than that of the capillary rheometer. This is because slip occurred in

the capillary and the apparent strain rate of capillary rheometer was higher than the wall strain rate of parallel plate rheometer.

On the other hand, Cox-Merz (1958) compared the viscosity of parallel plates rheometer by using the complex viscosity (η^*) and the frequency (ω) with the viscosity of capillary rheometer by using the viscosity (η') and the apparent strain rate ($\dot{\gamma}_a$). Their rule equates the magnitude of complex viscosity to the steady shear viscosity. The result is shown in figures 2.1(b), 2.2(b) and 2.3(b).

It is a pleasure to find that both the transformation equation and the Cox - Merz rule give nearly the same result for the viscosity. The data collapes well at the higher value of frequency (ω). The result may be fortuitous.

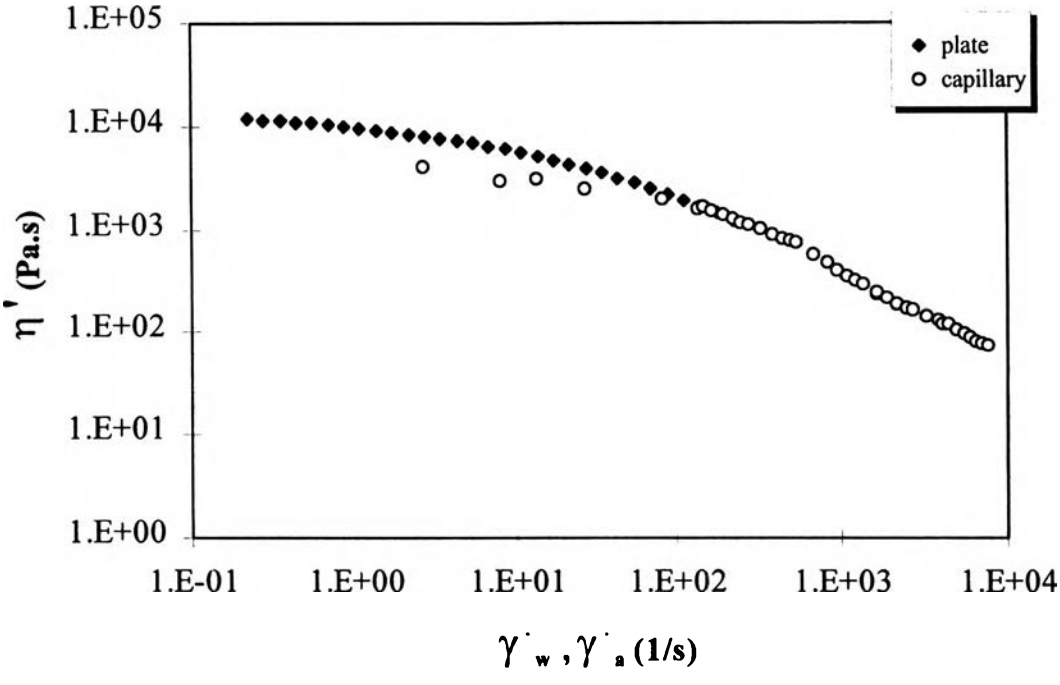

Figure 2.1(a) The viscosity vs. the wall the and apparent strain rate LLDPE (L1810F) by transformation at 185°C.

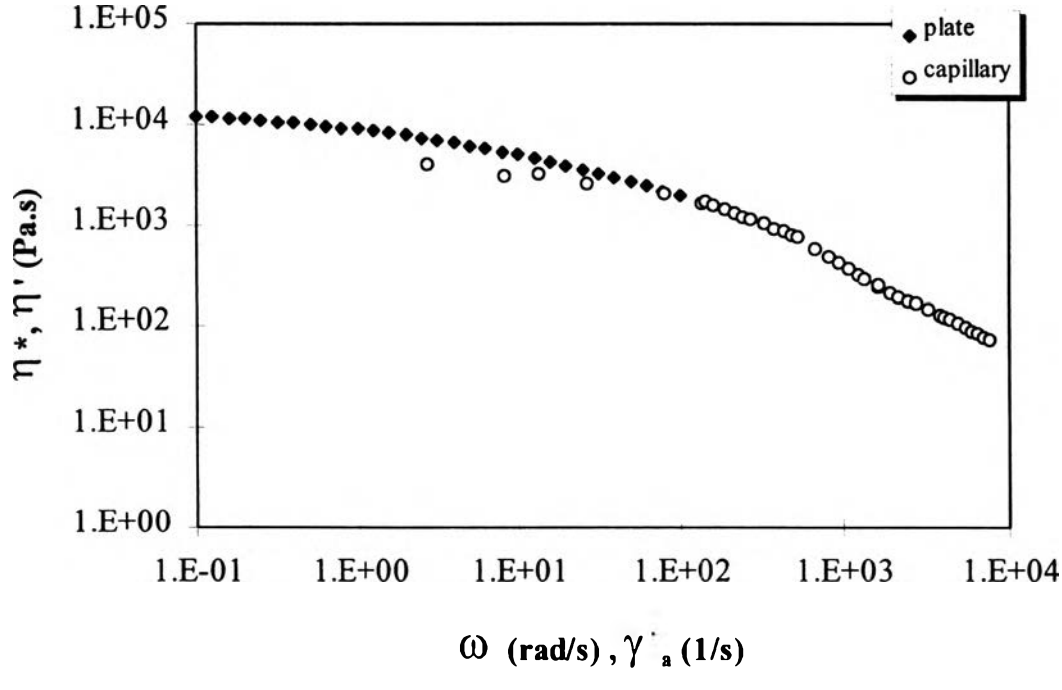

Figure 2.1(b) The viscosity vs. the apparent strain rate and frequency of LLDPE (L1810F) by the Cox - Merz rule at 185°C.

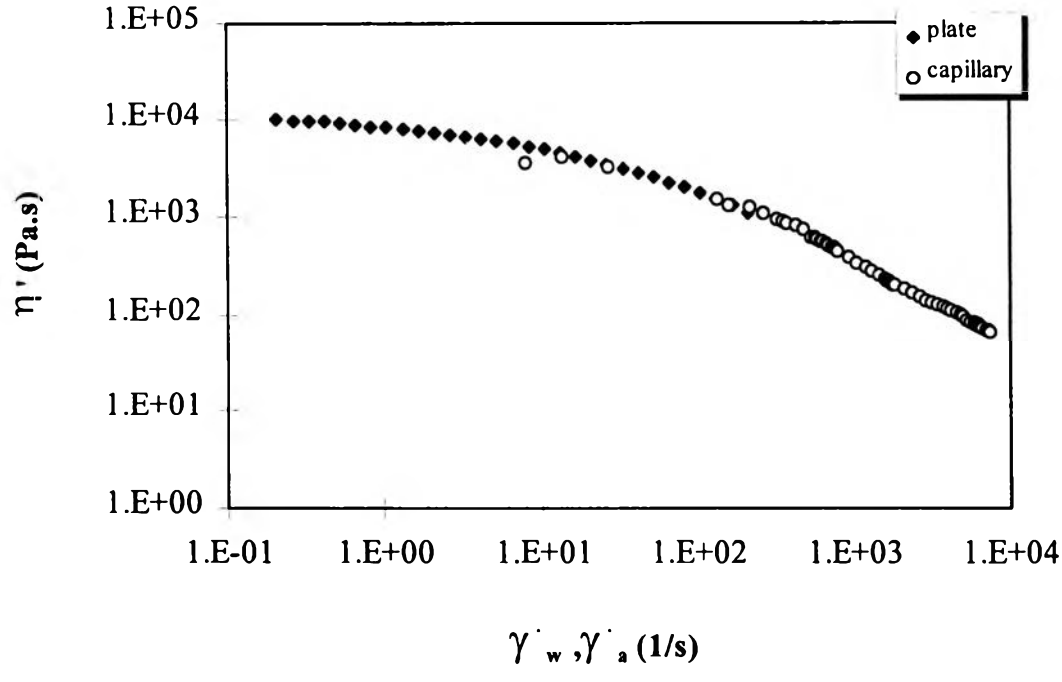

Figure 2.2(a) The viscosity vs. the wall the and apparent strain rate LLDPE (L2009F) by transformation at 185°C.

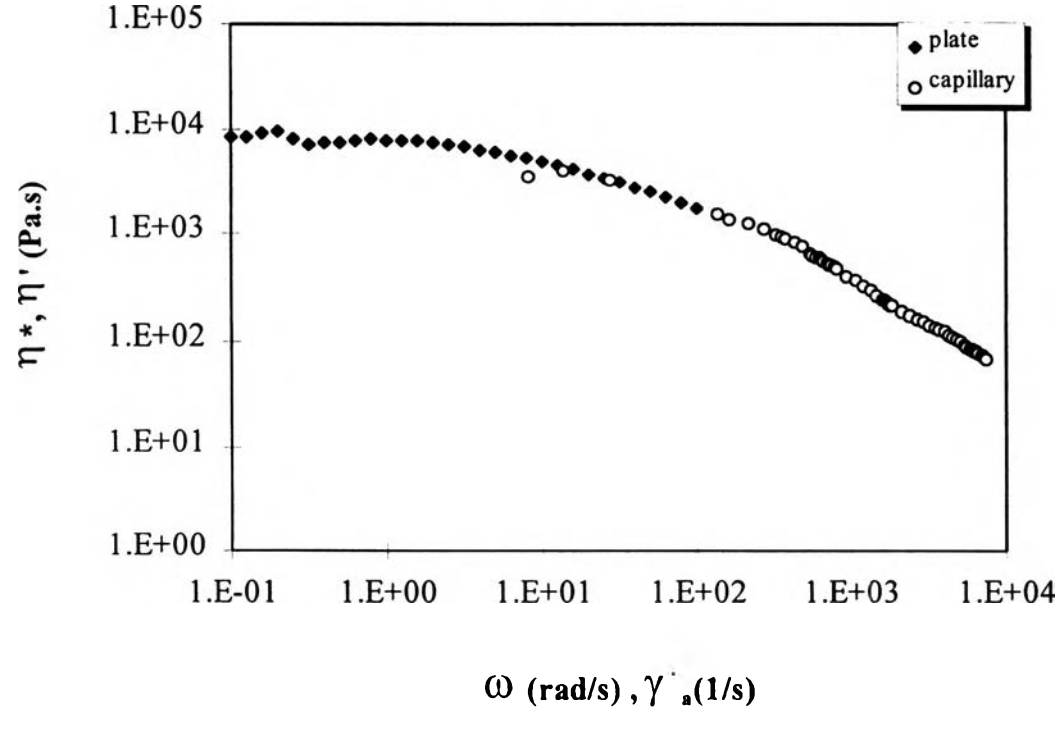

Figure 2.2(b) The viscosity vs. the apparent strain rate and frequency of LLDPE (L2009F) by the Cox - Merz rule at 185°C.

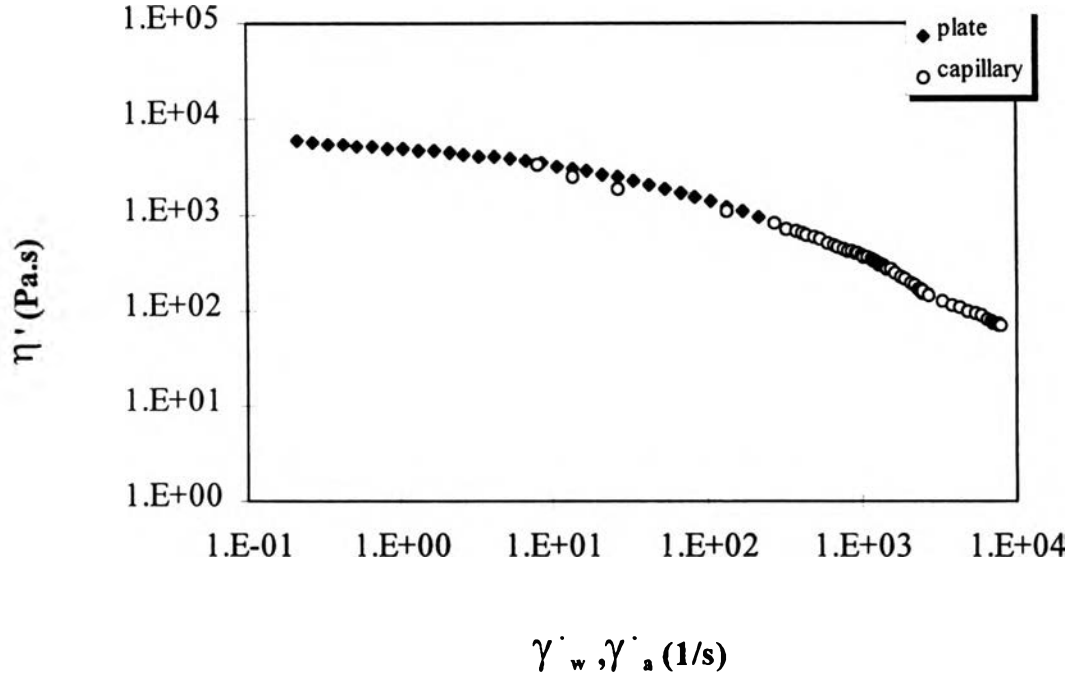

Figure 2.3(a) The viscosity vs. the wall the and apparent strain rate LLDPE (L2020F) by transformation at 185°C.

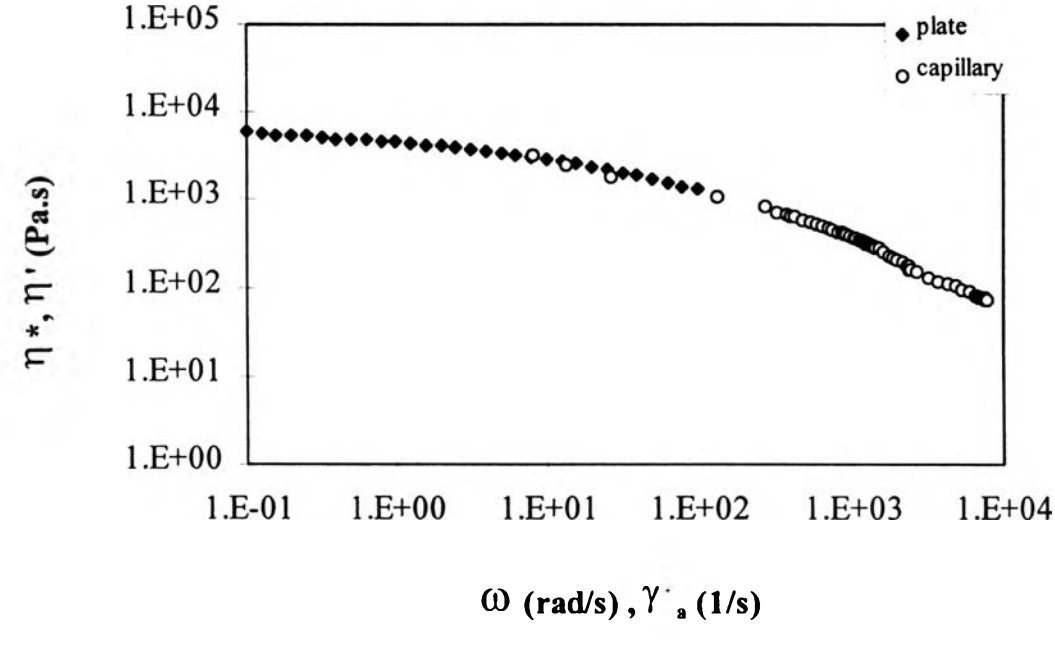

Figure 2.3(b) The viscosity vs. the apparent strain rate and frequency of LLDPE (L2020F) by the Cox - Merz rule at 185°C.

2.6 The Extrudate Surface and Sharkskin Studies

2.6.1 Zoom Stereo Microscopy

Zoom stereo microscope used was OLYMPUS BO71, with a magnification range of 4 - 80 times. The extrudates were examined at 20x magnification.

2.6.2 Optical Microscopy

Optical microscope used was OLYMPUS PM20, with a magnification range of 12.5 - 1,500 times. The extrudates were examined at 100 x magnification to detect a critical point of surface defect in each regime of the flow curves.

2.6.3 Scanning Electron Microscopy (SEM)

SEM was used JEOL 5200 - 2AE (MP152001), with a magnification range of 35 - 200,000 times. The sharkskin extrudates were examined at 200 x magnification to measure wavelengths (λ_S) and amplitudes (ε_S) of the sharkskin extrudates.